LAMINAR AND TURBULENT DISPERSION OF

MISCIBLE FLUIDS IN POROUS MEDIA

Submitted by

Harold D. Simpson

In partial fulfillment of the requirements

for the Degree of Master of Science

Colorado State University

Fort Collins, Colorado

June, 1969

COLORADO STATE UNIVERSITY

———

June, 1969

WE HEREBY RECOMMEND THAT THE THESIS PREPARED UNDER OUR SUPERVISION

BY HAROLD D. SIMPSON ENTITLED LAMINAR AND TURBULENT DISPERSION OF

MISCIBLE FLUIDS IN POROUS MEDIA BE ACCEPTED AS FULFILLING THIS PART OF

THE REQUIREMENTS FOR THE DEGREE OF MASTER OF SCIENCE.

Committee on Graduate Work

_____

_____

_____   _____
Adviser   Head of Department

Examination Satisfactory

Committee on Final Examination

_____

_____

_____   _____
                             Adviser

Permission to publish this thesis or any part of it
must be obtained from the Dean of the Graduate School

ABSTRACT

LAMINAR AND TURBULENT DISPERSION OF

MISCIBLE FLUIDS IN POROUS MEDIA

The phenomenon of longitudinal dispersion in the flow of miscible
fluids through porous media was studied in this investigation. The
relationship between the longitudinal dispersion coefficient and the
average pore velocity was found experimentally for the three regimes of
fluid flow in a porous medium.

An equation was developed describing the tracer concentration for
the continuous injection of a tracer fluid from a point source in a
column of porous medium. The experimental breakthrough curve was used
with this equation to find the longitudinal dispersion coefficient as
a function of average pore velocity.

Harold D. Simpson
Civil Engineering Department
Colorado State University
Fort Collins, Colorado, 80521
June, 1969

ACKNOWLEDGEMENTS

TABLE OF CONTENTS

LIST OF FIGURES

Chapter I

INTRODUCTION

The Problem of Dispersion in Nonlinear Flow

Consider the flow of a fluid through a bed of porous medium and let the composition of the fluid suddenly change at the source so that there are now two miscible fluids flowing through the porous medium. There will be a band of mixed fluid between the two pure fluids with the length of this band being dependent on longitudinal dispersion (mixing in the direction of the mean flow velocity). The longitudinal dispersion is due primarily to the hydrodynamic mixing of the fluids as they flow through the porous medium and is a function of the velocity of the fluids in the porous medium and of the physical properties of the porous medium.

Longitudinal dispersion of miscible fluids in flow through porous media has been researched considerably in the laminar flow regime where Darcy's law is valid. There has been no research found by this writer which was aimed particularly at the transitional and nonlinear regimes of flow. Therefore, it was thought desirable to investigate longitudinal dispersion in all three regimes of flow.

The dispersion phenomenon is important to the petroleum industry because of its affect on the miscible displacement process used in secondary recovery operations. Dispersion of heat and mass is also a factor that must be considered in the design and operation of fixed bed continuous mixing apparatus such as chemical reactors, distillation

columns, extractor columns, heat exchangers, and rotary mixers (12).*

These fixed or packed bed apparatus often attain nonlinear flow conditions especially near walls (3).

Scope of the Investigation

This investigation will be limited to a laboratory study of longitudinal dispersion in porous media. A relationship between longitudinal dispersion D_L ** and average velocity $\bar{w}$ will be shown for various sizes of sand d_p. The value of the average velocity $\bar{w}$ will cover three orders of magnitude and also will include the three regimes of flow: laminar, transitional, and nonlinear.***

The equation necessary to analyze the laboratory data will be developed for the boundary conditions of the apparatus used.

---

* Numbers in parentheses refer to references in the bibliography.

** A complete list of symbols and their units is given in Appendix A.

*** The term nonlinear will be used to describe flow conditions where Darcy's law is not valid. The term turbulent is often used to describe nonlinear flow conditions also.

Chapter II

LITERATURE REVIEW

Investigation of the dispersion phenomenon that occurs when there
is flow of two miscible fluids in a porous medium dates back to the
beginning of this century when Slichter (20) studied the underground
movement of water using an electrolyte tracer. He observed that the
tracer, when injected from an upstream well, did not reach a downstream
observation well as a sharp front but was dispersed in the form of an
S-shaped curve. This S-shaped curve is often called the breakthrough
curve of the tracer fluid and is obtained by plotting concentration of
the tracer versus time from injection (See Figure 1). Slichter postu-
lated that the breakthrough curve was due to the fact that the tracer
fluid flowing in the center of the pores of the soil structure moves
faster than that flowing near the pore wall. Thus some of the tracer
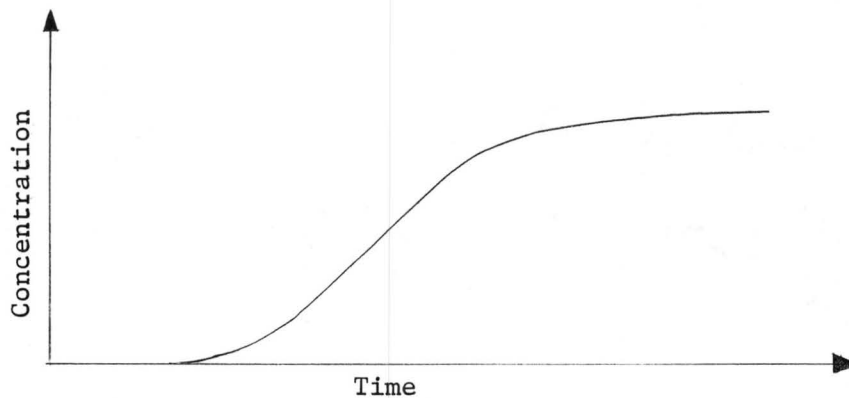particles reached the observation well sooner than others.

Figure 1. Breakthrough Curve

The longitudinal dispersion coefficient D_L is the sum of the effect of hydrodynamic mixing due to fluid flow and of the effect of molecular diffusion which results from the contact of two miscible fluids. Ordinarily the diffusion term is very insignificant except for very low velocities.

When two miscible fluids are in contact along a plane interface, they will slowly diffuse into each other according to the following differential equation (4)

$$\frac{\partial c}{\partial t} = F \frac{\partial^2 c}{\partial x^2} \tag{1}$$

where

c = concentration of the tracer fluid (mg/1)

F = molecular diffusion coefficient (sq. cm/sec)

t = time (seconds)

x = length in x direction (cm).

The term F is dependent upon the two fluids present and usually is considered independent of concentration in equation 1. It is also independent of fluid movement due to velocity convection. The longitudinal dispersion coefficient has been defined as (16)

$$D_L = D + F \tag{2}$$

where D is associated with hydrodynamic mixing only.

Equation 1 is derived by considering the mass-balance of a volume element. The mass flux through an area is proportional to the concentration gradient normal to that area and the diffusion coefficient F.

If this mass flux is applied to the continuity equation, the result is equation 1 for a concentration gradient in the x direction only.

Kitagowa (11) in 1935 first studied the dispersion phenomena as a separate problem. Experimental results on the dispersion of a sodium chloride tracer from a point source in horizontal flow were reported. The results indicated that the tracer concentration or breakthrough curve varied as a normal probability curve. Kitagowa also stated that the coefficient of dispersion was directly proportional to large average velocity $\bar{v}$ of flow and inversely proportional to $\bar{v}$ for very low average velocity.

After Kitagowa's data showed that the breakthrough curve had a form of the normal probability law, several investigators presented theories using the mathematics of probability as the basis for their work.

P. V. Danckwerts (5) considered a packed tube of length L through which fluid A flows with mean velocity $\bar{w}$. At time t = 0 the flow is changed to another fluid B which is miscible with fluid A. He stated that if the flow was of the piston type, the plane interface of the two fluids would move through the tube with the mean velocity $\bar{w}$. This imaginary plane interface was taken as the axis of the co-ordinate system. Then the velocity of any element of fluid relative to the axis x = 0 would fluctuate irregularly. At times the fluid element would be near a solid surface where viscous forces would slow it down. While at other times the element would be near the center of a channel where the velocity would be greater than the mean. He stated that if the packing was randomly arranged, each fluid element

would travel at the same average velocity and would experience fluctuations of the same average magnitude and frequency.

He used the "random walk" theory to describe this behavior. The result was the redistribution of fluid A and fluid B according to the equation of diffusion,

$$\frac{\partial c}{\partial t} = D_L \frac{\partial^2 c}{\partial x^2} \tag{3}$$

The D_L was called "diffusivity" but actually is the coefficient of longitudinal dispersion as defined in equation 2.

The "random walk" theory postulates that a particle undergoes a displacement from its starting position of

$$S_n = \sum_{i=1}^{n} x_i \tag{4}$$

after n steps where each x_i is an independent random variable. S_n will have a mean and variance, respectively of

$$x = \frac{\sum x_i}{n} = 0 \tag{5}$$

and
$$\sigma^2 = \frac{2D_L t}{n} \quad . \tag{6}$$

If n is large, then S_n is normally distributed in the sense that the "central limit theorem of probability" holds. The normal probability density function of S_n is then given by

$$p_{sn}(x) = \left(\frac{1}{2\pi\sigma^2 n}\right)^{1/2} \exp - (x^2/2\sigma^2 n). \tag{7}$$

The basis for equations in this paragraph was taken from Parzen (14). Figure 2 is a graph of a normal density function.

$$p(x) = \frac{1}{\sqrt{2\pi}} \exp - (x^2/2)$$

with
$$\bar{x} = 0$$
$$\sigma = 1$$
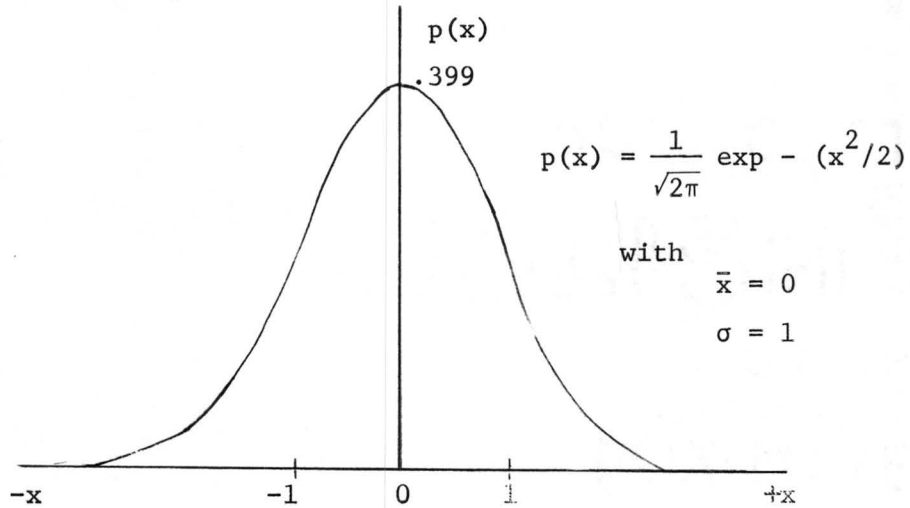
Figure 2. Normal Density Function

If equation 6 is substituted into equation 7, the result is

$$p_{sn}(x) = \frac{1}{\sqrt{4\pi D_L t}} \exp - (x^2/4D_L t) \quad . \tag{8}$$

Let the probability density function of S_n be replaced by a probability density function of the concentration c. The probability density function of c must be integrated from $x = -\infty$ to $x = +\infty$ to give the corresponding distribution function of the concentration c for all x. The boundary conditions pertaining to Danckwerts' dispersion model are:

$$c/c_o = 0 \qquad x > 0 \qquad t = 0$$
$$c/c_o = 1 \qquad x < 0 \qquad t = 0 \tag{9}$$

$$c/c_o = 0 \qquad x = + \infty \qquad t > 0$$
$$c/c_o = 1 \qquad x = - \infty \qquad t > 0.$$

When these boundary conditions are applied to the integration of equation 8, the result is

$$\frac{c}{c_o} = \frac{1}{2} \left[1 - \text{erf} \left(\frac{L - \bar{w}t}{2\sqrt{D_L t}} \right) \right] \tag{10}$$

where

$$\text{erf} (a) = \frac{2}{\sqrt{\pi}} \int_o^a e^{-y^2} dy \quad .$$

Equation 10 describes the tracer breakthrough curve at the outlet of the column as a function of time (See Figure 1). The error function (erf) is tabulated for values of α and can be used to solve equation 10 for D_L.

A. E. Scheidegger (17) in 1953 applied the statistics of disordered phenomena to the flow of fluids through porous media. This had not been done before on such a strict statistical basis. He explained however that the flow of fluids through porous media is not a stochastic process but is completely determined by the equations of motion and boundary conditions. His fundamental idea was to consider a great number of small volumes of a particular porous medium with identical macroscopic properties. In this way it is possible to define "ensemble averages" or "probabilities" for which the probability distribution function may be written. The final result of his work was an equation for the fundamental probability distribution describing the journey of a fluid particle through the porous medium. The equation is based on the following assumptions:

a) The porous medium is homogeneous and isotropic.
b) The external forces acting on the fluid are homogeneous and time independent.
c) Different parts of a sample are macroscopically identical.

The equation is

$$P(z,t) = \frac{1}{\sqrt{4\pi D_L t}} \exp - \frac{(z - \bar{z})^2}{4D_L t} \tag{11}$$

where $\bar{z} = \bar{w}t$ and z corresponds to the vertical axis.

The variance was defined as

$$\sigma^2 = 2D_L t \tag{12}$$

where σ is the standard deviation. Thus the standard deviation or "spread" increases with the square root of time t. Equation 11 is the same as equation 8 with $x = z - \bar{z}$.

P. R. Day (6) used the results of Scheidegger's paper and applied it to specific types of dispersion problems. Day described various methods of injection of a sodium chloride solution into steady laminar flow of water through a column of saturated sand. He developed equations describing the variation of the tracer concentration with time for each of the methods.

Day clarified Scheidegger's work with regard to "ensemble averages" or "probabilities." He made the distinction between true streamlines and conventional streamlines which are commonly used to describe flow in a porous medium. Conventional streamlines are drawn tangent to average velocity vectors while true streamlines are everywhere tangent to actual velocity vectors. True streamlines are much

more complicated geometrically because they may intertwine as they pass through the porous medium.

Day discussed a "cluster" of fluid particles as it moved through the porous medium. A cluster of many particles would follow a composite path which would be simpler than the paths of the individual particles. The center of the cluster would move along the conventional streamlines with the average velocity $\bar{w}$. However due to the flow geometry of the actual streamlines, the particles of the cluster will be hydrodynamically dispersed because some particles would take longer paths of flow while others would take shorter paths.

The equation describing the probability that a given particle after a time t will be found in the pore volume element ∂V located a distance r along any diameter passing through the expected position of the cluster at that time is

$$P\partial V = (4\pi D_L t)^{-3/2} \exp [-r^2/4D_L t] \, \partial V \quad . \qquad (13)$$

The particles of the cluster are distributed along any diameter according to the normal density function with the maximum at the center (see Figure 2).

Equation 13 was then used to derive the equation describing the flow of a small volume of tracer at initial concentration c_o injected instantaneously at the inlet of a column of sand with water flowing through it. The result was

$$\frac{c}{c_o} = \frac{V_o}{(4\pi D_L t)^{3/2}} \exp [-r^2/4D_L t] \qquad (14)$$

where V_o is the volume of sand required to contain the volume of tracer fluid injected. If the concentration of the tracer can be measured, then equation 14 could be used to find the longitudinal dispersion coefficient D_L by a trial and error method of curve fitting.

Day also presented an equation describing the dispersion of salt water that totally displaces fresh water across the whole sand column. The result was the same as Danckwerts, that is equation 10. Day did not present any results except to show that Scheidegger's analysis did describe the actual flow of a tracer fluid through a porous medium.

Rifai (16) developed the same probability distribution equation as did Scheidegger but from a slightly different approach. He applied equation 11 to the dispersion of an interface of two miscible fluids moving with average velocity $\bar{w}$. The result was equation 10 which is for the case of the coordinate system moving with the average velocity $\bar{w}$.

He then considered the case of the coordinate system located at the entrance of the sand column for the same conditions as in the above paragraph. The differential equation describing the rate of change of concentration due to flow in the z direction only of a tracer fluid was shown to be

$$\frac{\partial c}{\partial t} = D_L \frac{\partial^2 c}{\partial z^2} - \bar{w} \frac{\partial c}{\partial z} \quad . \tag{15}$$

The first term on the right-hand side of equation 15 represents the motion of the tracer due to longitudinal dispersion and molecular diffusion while the second term is due to velocity convection. The negative sign is due to the fact that $\partial c/\partial z$ is negative (see Figure 3).
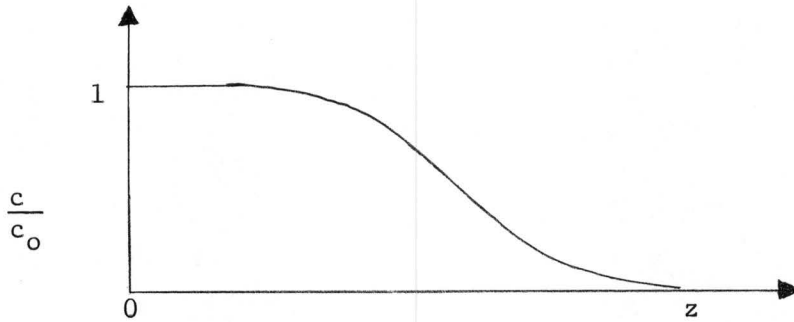
Figure 3. Concentration versus Distance Curve

Rifai solved the partial differential equation (equation 15) for the boundary conditions and initial conditions in equation 9. He found after going through a rigorous analysis that the solution to equation 15 differed from equation 10 by the factor

$$\exp\left(\frac{\bar{w}z}{D_L}\right) \quad \left[\mathrm{erfc}\left(\frac{z + \bar{w}t}{2\sqrt{D_L t}}\right)\right] .$$

This factor was found by Rifai in actual computation to be very small, on the order of 0.001, and thus could be neglected. Thus equation 10 was used to determine the longitudinal dispersion coefficient D_L.

Some of the results of Rifai's work were that D_L was independent of length of flow if the porous medium was homogeneous and that D_L was approximately proportional to the average velocity $\bar{w}$. The actual relationship between D_L and $\bar{w}$ for an Ottawa sand and a non-uniform Monterey sand was, respectively,

$$D_L = 0.063\, \bar{w}^{1.02} \tag{16a}$$

and

$$D_L = 0.013\, \bar{w}^{1.18} . \tag{16b}$$

The maximum average velocity of flow for both cases was 0.2 cm/sec. The constant coefficient multiplier of the velocity term was found to be mainly a function of the porous medium.

Other investigators have found similar results for the laminar regime. Ebach and White (7) found for a range of velocities of 0.3 cm/sec to 3. cm/sec that

$$D_L = a \; \bar{w}^{1.10} \tag{17}$$

was valid for spheres ranging in size from 1.0 mm to 3.4 mm. The coefficient a increased with increase in sphere diameter. Harleman and others (9) found for a range of velocities of 0.01 cm/sec to 0.15 cm/sec that

$$D_L = a \; \bar{w}^{1.20} \tag{18}$$

was valid for sands and spheres ranging in size from 0.45 mm to 2. mm. The coefficient a increased with increase in particle size and was larger for the sand than for the smoother spheres.

Investigators, especially in the chemical engineering field, report the results of their longitudinal dispersion studies in terms of the longitudinal Peclet number Pe_L where

$$Pe_L = d_p \; \bar{w}/D_L \quad . \tag{19}$$

Most of these investigators show their results as a plot of Pe_L versus Reynolds number R on a log-log graph where

$$R = d_p \; \bar{w} \; \rho/\mu \quad . \tag{20}$$

Several of these investigators show theoretically that for very high Reynolds number that the longitudinal Peclet number should approach a constant value of 2.0 (2, 13). This would mean theoretically, using equation 19, that

$$D_L = d_p \, \bar{w} \, / \, 2.$$
(21)

or in other words that D_L is proportional to the average velocity $\bar{w}$ for the nonlinear flow regime.

There has been one study of the dispersion phenomenon in porous media for the nonlinear regime of flow. Bernard and Wilhelm (3) investigated the radial dispersion coefficient D_R for the nonlinear regime. The laboratory dispersion apparatus used a method of tracer injection called the point source type. This meant that the tracer solution was injected into the flow from a small tube located on the centerline of a much larger tube packed with porous media.

The tracer solution was continuously injected and concentration measurements were made radially from the center of the tube at a distance L downstream. The measurement of concentration was made after the concentration gradient associated with longitudinal dispersion had passed through the column.

For high Reynolds number, the radial Peclet number approached a value of 11. To attain the high Reynolds number, particles used for the porous medium had grain sizes of 5. mm to 8. mm. This particular investigation was included in the literature review because its method of injection is similar to the type used in this study.

From the previous paragraphs, it can be seen that the investigation of longitudinal dispersion has been largely confined to the

laminar flow regime with theory developed for the nonlinear regime.
The reasons for the lack of investigations in the nonlinear regime are
either the lack of laboratory equipment to attain the high velocities
necessary or the lack of an equation describing the flow of the tracer
fluid for an injection method that must be used to attain the high
velocities.

Chapter III

DEVELOPMENT OF THEORY

The method of tracer fluid injection to be used in this investigation will be the point source type. With this method there will be concentration gradients in both the longitudinal and radial directions with respect to flow direction. Therefore the equation describing the probability distribution of a "cluster" of tracer particles must include the effect of radial dispersion.

Rifai (16) and Scheidegger (17) have developed the probability distribution for the case of three dimensional flow of a tracer fluid cluster in the x, y, and z directions. If this equation is rewritten in cylindrical coordinates for flow in the z direction only, the result is

$$P(z,r,t) = \frac{1}{(4\pi t)^{3/2} \, D_L^{1/2} D_R} \exp\left\{-[r^2 + \frac{D_R}{D_L}(z-\bar{w}t)^2]/4D_R t\right\} \quad (22).$$

Equation 22 can be related to the physical situation of the flow of a small volume of tracer fluid injected almost instantly. This can be done in the same way as did Day (6). The result is

$$c = \frac{c_o V}{(4\pi t)^{3/2} \, D_L^{1/2} D_R} \exp\left\{-[r^2 + \frac{D_R}{D_L}(z-\bar{w}t)^2]/4D_R t\right\} \quad (23)$$

where V is the volume of tracer solution injected with the initial concentration c_o.

The partial differential equation describing the flow of a
tracer fluid when injected from a point source into one dimensional
flow with the cylindrical coordinate system located at the column inlet
is

$$\frac{\partial c}{\partial t} = D_L \frac{\partial^2 c}{\partial z^2} + D_R \left[\frac{\partial^2 c}{\partial r^2} + \frac{1}{r} \frac{\partial c}{\partial r} \right] - \bar{w} \frac{\partial c}{\partial z} \ . \tag{24a}$$

Hoopes and Harleman (10) solved equation 24a for the case of an in-
stantaneous injection of a small volume of tracer fluid. The boundary
and initial conditions used for the solution are as follows:

$$
\begin{array}{llll}
c = c_o V & r = 0 & z = 0 & t = 0 \\
c = 0 & r > 0 & z > 0 & t < 0 \\
c = 0 & r = \infty & z > 0 & t > 0 \\
c = 0 & r > 0 & z = \infty & t > 0
\end{array}
\tag{24b}
$$

$c_o V$ is the mass of the tracer injected.

The solution ot equation 24a was found to be exactly the same as
equation 23. The solution was found by using a method from the heat
flow technology.

In this investigation, the tracer fluid will be injected con-
tinuously under steady one dimensional flow conditions. Therefore the
mass of tracer injected in a time Δt is $c_o Q \Delta t$ where Q is the flow rate
of the tracer fluid at z = 0 and r = 0. The change in concentration
Δc at a point r, z due to an increment of mass $c_o Q \Delta t$ is

$$\Delta c = \frac{c_o Q \Delta t}{(4\pi t)^{3/2} D_L^{1/2} D_R} \ \exp \left\{ - \left[r^2 + \frac{D_R}{D_L} (z - \bar{w}t)^2 \right] / 4 D_R t \right\} \ . \tag{25}$$

Equation 25 must be integrated from time t = 0 to time t = t'
in order that the concentration c at a point z and r at time t' can be

found for continuous injection of a tracer fluid. Integrating equation 25 results in

$$\frac{c}{c_o} = \frac{Q}{(4\pi)^{3/2} D_L^{1/2} D_R} \int_0^{t'} \exp\left\{-[r^2 + \frac{D_R}{D_L}(z-\bar{w}t)^2]/4D_R t\right\} \frac{dt}{t^{3/2}} \qquad (26)$$

or upon rearrangement

$$\frac{c}{c_o} = \frac{Q}{(4\pi)^{3/2} D_L^{1/2} D_R} \int_0^{t'} \exp\left\{-\left[\frac{r^2}{4D_R t} + \frac{z^2 D_R/D_L}{4D_R t} + \frac{\bar{w}^2 t}{4D_L} - \frac{\bar{w}z}{2D_L}\right]\right\} \frac{dt}{t^{3/2}} \qquad (27)$$

Setting

$$\eta = \sqrt{r^2 + \frac{D_R}{D_L} z^2} \qquad (28)$$

and substituting into equation 27 results in

$$\frac{c}{c_o} = \frac{Q \exp\left(\frac{\bar{w}z}{2D_L}\right)}{(4\pi)^{3/2} D_L^{1/2} D_R} \int_0^{t'} \exp\left\{-\left[\frac{\eta^2}{4D_R t} + \frac{\bar{w}^2 t}{4D_L}\right]\right\} \frac{dt}{t^{3/2}} \qquad (29)$$

Now changing the variable of integration by letting

$$\Sigma = \frac{\eta}{\sqrt{4D_R t}} = \eta(4D_R t)^{-1/2} \qquad , \qquad (30)$$

the derivative with respect to time t is

$$\frac{d\Sigma}{dt} = \frac{-\eta}{4D_R^{1/2} t^{3/2}} \qquad . \qquad (31)$$

The limits of the integral in terms of the new variable are:

$$\text{lower limit as } t \to 0 \text{ , } \quad \Sigma = \frac{\eta}{\sqrt{4D_R t'}} = \infty$$

$$\text{upper limit for } t = t' \text{ , } \quad \Sigma = \frac{\eta}{\sqrt{4D_R t'}} \quad .$$

Equation 29 becomes after substitution of equations 30 and 31

$$\frac{c}{c_o} = \frac{4Q \exp\left(\frac{\bar{w}z}{2D_L}\right)}{\eta (4\pi)^{3/2} D_L^{1/2} D_R^{1/2}} \int_{\infty}^{\eta/\sqrt{4D_R t'}} -\exp\left\{-\left[\Sigma^2 + \frac{\bar{w}\eta^2}{\Sigma^2 D_L D_R 16}\right]\right\} d\Sigma \tag{32}$$

To obtain a solution that can be easily worked with, the above integral can be rearranged in terms of the complementary error function (erfc) which is equal to the term 1. - erf. The upper limit of the integral must be ∞ so that the erfc can be developed. Using the definitions

$$\int_a^b = - \int_b^a \tag{33a}$$

and

$$\text{erfc } (a) = \frac{2}{\sqrt{\pi}} \int_a^\infty e^{-y^2} dy \quad , \tag{33b}$$

equation 32 becomes

$$\frac{c}{c_o} = \frac{Q \exp\left(\frac{\bar{w}z}{2D_L}\right)}{2\eta\pi^{3/2} D_L^{1/2} D_R^{1/2}} \int_{\eta/\sqrt{4D_R t'}}^{\infty} \exp-\left[\Sigma^2 + \frac{\bar{w}^2\eta^2}{16\Sigma^2 D_L D_R}\right] d\Sigma \quad . \tag{34}$$

The exponent in the integral can be rewritten in the form of a perfect square, and equation 34 becomes

$$\frac{c}{c_o} = \frac{Q \, \exp\left(\frac{\bar{w}z}{2D_L}\right)}{2\eta\pi^{3/2}D_L^{1/2}D_R^{1/2}} \left\{ \exp\left(\frac{\bar{w}\eta}{2\sqrt{D_L D_R}}\right) \int_{\eta/\sqrt{4D_R t'}}^{\infty} \exp - \left[\left(\Sigma + \frac{\bar{w}\eta}{4\Sigma\sqrt{D_R D_L}} \right)^2 \right] d\Sigma \right\} . \quad (35)$$

Equation 35 can now be rewritten in an equivalent form so that another change of variable will result in a form of the erfc integral. Equation 35 becomes

$$\frac{c}{c_o} = \frac{Q \, \exp\left(\frac{\bar{w}z}{2D_L}\right)}{2\eta\pi^{3/2}D_L^{1/2}D_R^{1/2}} \left\{ \frac{\exp\left(\frac{\bar{w}\eta}{2\sqrt{D_L D_R}}\right)}{2} \int_{\eta/\sqrt{4D_R t'}}^{\infty} \left(1 - \frac{\bar{w}\eta}{4\Sigma^2\sqrt{D_R D_L}} \right) \exp \right.$$

$$- \left(\Sigma + \frac{\bar{w}\eta}{4\Sigma\sqrt{D_L D_R}} \right)^2 d\Sigma + \frac{\exp -\left(\frac{\bar{w}\eta}{2\sqrt{D_L D_R}}\right)}{2} \int_{\eta/\sqrt{4D_R t'}}^{\infty} \left(1 + \frac{\bar{w}\eta}{4\Sigma^2\sqrt{D_R D_L}} \right) \exp$$

$$\left. - \left(\Sigma - \frac{\bar{w}\eta}{4\Sigma\sqrt{D_L D_R}} \right)^2 d\Sigma \right\} . \quad (36)$$

A change of the variable of integration can be made by letting

$$\alpha = \Sigma + \frac{\bar{w}\eta}{4\Sigma\sqrt{D_L D_R}} \quad (37)$$

and

$$\beta = \Sigma - \frac{\bar{w}\eta}{4\Sigma\sqrt{D_L D_R}} \quad (38)$$

and with the derivative with respect to Σ of α and β being

$$\frac{d\alpha}{d\Sigma} = 1 - \frac{\bar{w}\eta}{4\sqrt{D_R D_L}\Sigma^2} \quad , \tag{39}$$

and

$$\frac{d\beta}{d\Sigma} = 1 + \frac{\bar{w}\eta}{4\sqrt{D_R D_L}\Sigma^2} \quad . \tag{40}$$

The limits of the integrals in equation 36 become using equations 37 and 38 respectively,

lower limits:

$$\alpha_1 = \frac{\eta}{\sqrt{4D_R t'}} + \frac{\bar{w}t'}{\sqrt{4D_L t'}} \tag{41}$$

$$\beta_1 = \frac{\eta}{\sqrt{4D_R t'}} - \frac{\bar{w}t'}{\sqrt{4D_L t'}} \tag{42}$$

upper limits:

$$\alpha_2 = \beta_2 = \infty \quad .$$

Substituting equations 37, 38, 39, 40, 41, and 42 into equation 36, results in

$$\frac{c}{c_o} = \frac{Q \exp\left(\frac{\bar{w}z}{2D_L}\right)}{2\eta\pi^{3/2}D_L^{1/2}D_R^{1/2}} \left\{ \frac{\exp\left(\frac{\bar{w}\eta}{2\sqrt{D_L D_R}}\right)}{2} \int_{\frac{\eta}{\sqrt{4D_R t'}} + \frac{\bar{w}t'}{\sqrt{4D_L t'}}}^{\infty} \exp-(\alpha)^2 d\alpha \right.$$

$$\left. + \frac{\exp\left(-\frac{\bar{w}\eta}{2\sqrt{D_L D_R}}\right)}{2} \int_{\frac{\eta}{\sqrt{4D_R t'}} - \frac{\bar{w}t'}{\sqrt{4D_L t'}}}^{\infty} \exp-(\beta)^2 d\beta \right\} . \tag{43}$$

Using the definition of the complementary error function (equation 33b),
equation 43 becomes

$$\frac{c}{c_o} = \frac{Q \exp\left(\frac{\bar{w}z}{2D_L} - \frac{\bar{w}\eta}{2\sqrt{D_L D_R}}\right)}{8\eta\pi D_L^{1/2} D_R^{1/2}} \left\{ \exp\left(\frac{\bar{w}\eta}{\sqrt{D_L D_R}}\right) \text{erfc}\left[\frac{\eta}{\sqrt{4D_R t'}} + \frac{\bar{w}t'}{\sqrt{4D_L t'}}\right] \right.$$

$$\left. + \text{erfc}\left[\frac{\eta}{\sqrt{4D_R t'}} - \frac{\bar{w}t'}{\sqrt{4D_L t'}}\right] \right\} . \tag{44}$$

Now if the concentration is measured at the centerline, r = 0,
then η becomes

$$\eta = \sqrt{\frac{D_R}{D_L} z^2} . \tag{45}$$

Putting this value into equation 44 results in the following expression
for the concentration of the tracer fluid at the centerline for any z,

$$\frac{c}{c_o} = \frac{Q}{8\pi D_R z} \left\{ \text{erfc}\left(\frac{z - \bar{w}t'}{\sqrt{4D_L t'}}\right) + \exp\left(\frac{\bar{w}z}{D_L}\right) \text{erfc}\left(\frac{z + \bar{w}t'}{\sqrt{4D_L t'}}\right) \right\} . \tag{46}$$

The second term in the brackets of equation 46 is the identical
term that Rifai (16) found to be on the order 0.001 for actual compu-
tation. Therefore the breakthrough curve for r = 0 can be described
accurately by the following equation

$$\frac{c}{c_o} = \frac{Q}{8\pi D_R z} \left\{ \text{erfc}\left(\frac{z - \bar{w}t'}{\sqrt{4D_L t'}}\right) \right\} . \tag{47}$$

It must be noted that there still are two unknown variables in
the above equation, D_L and D_R. This problem can be circumvented by

treating the term

$$\frac{Q}{8\pi D_R z} = A$$

for each velocity $\bar{w}$ that D_L is being measured. The value of this constant A can be calculated from the experimental breakthrough curve. The midpoint of the breakthrough curve moves with the average velocity $\bar{w}$ and for a particular position z would reach it in time $t_m = z / \bar{w}$. Therefore at the midpoint the value of $z - \bar{w}t$ would be 0. and the erfc (0) is 1.0. Therefore the term A would equal c/c_0 or expressing it in another way, c at the midpoint would equal $c_0 A$. The concentration at the midpoint c_m corresponding to $t_m = z / \bar{w}$ would decrease with distance traveled according to

$$c_m = \frac{c_0 Q}{8\pi D_R z} \, . \tag{48}$$

If another value of concentration c_2 is used from the experimental breakthrough curve at a different time t_2, equation 47 becomes

$$\frac{c_2}{c_m} = \text{erfc} \left(\frac{z - \bar{w}t_2}{\sqrt{4D_L t_2}} \right) = \text{erfc}(b) \, . \tag{49}$$

The only unknown in equation 49 is D_L which can be calculated with the use of a table of the erfc. The ratio of c_2/c_m gives the value of erfc (b). The value of b can be found from the erfc tables and set equal to

$$b = \frac{z - \bar{w}t_2}{\sqrt{4D_L t_2}} \, . \tag{50}$$

The longitudinal dispersion coefficient D_L becomes

$$D_L = \left(\frac{z - \bar{w}t_2}{2b\sqrt{t_2}} \right)^2 \quad .$$

(51)

Now since a method of determining the longitudinal dispersion coefficient D_L for the continuous point source injection method has been developed for steady state, one dimensional flow, the relationship between D_L and average pore velocity $\bar{w}$ for the three regimes of flow will be investigated experimentally.

Chapter IV

LABORATORY INVESTIGATION

The entire experimental setup is shown in figure 4. The setup
will be divided into its functional sections and each section discussed
separately.

The fresh water supply is obtained from Horsetooth Reservoir
which provides a constant head source of up to 162 feet of water or
70 psi. The flow is delivered from the main 24 inch line by a 2.5 inch
line and is controlled by gate valve A. (All capital letters pertain
to figure 4.) The line pressure can be increased by 40 psi with the
use of a high pressure centrifugal pump B.

The flow rate is measured with one of three Fischer and Porter
flow meters C or an one inch orfice meter D for flow rates above
those of the flow meters. The three flow meters have a range of 0.0
to 430. cubic centimeters per second. A water column manometer is
used in conjunction with the orfice meter.

Pressure drop data is taken using a water column manometer and a
differential mercury manometer E. Pressure drop data is used to define
the regimes of flow. Four pressure taps are spaced as shown in figure
5. The four taps are used for two reasons. One is to determine if
the porous medium was packed uniformly along its length and the other
was to provide a means of keeping the pressure differential within
the limits of the manometers.
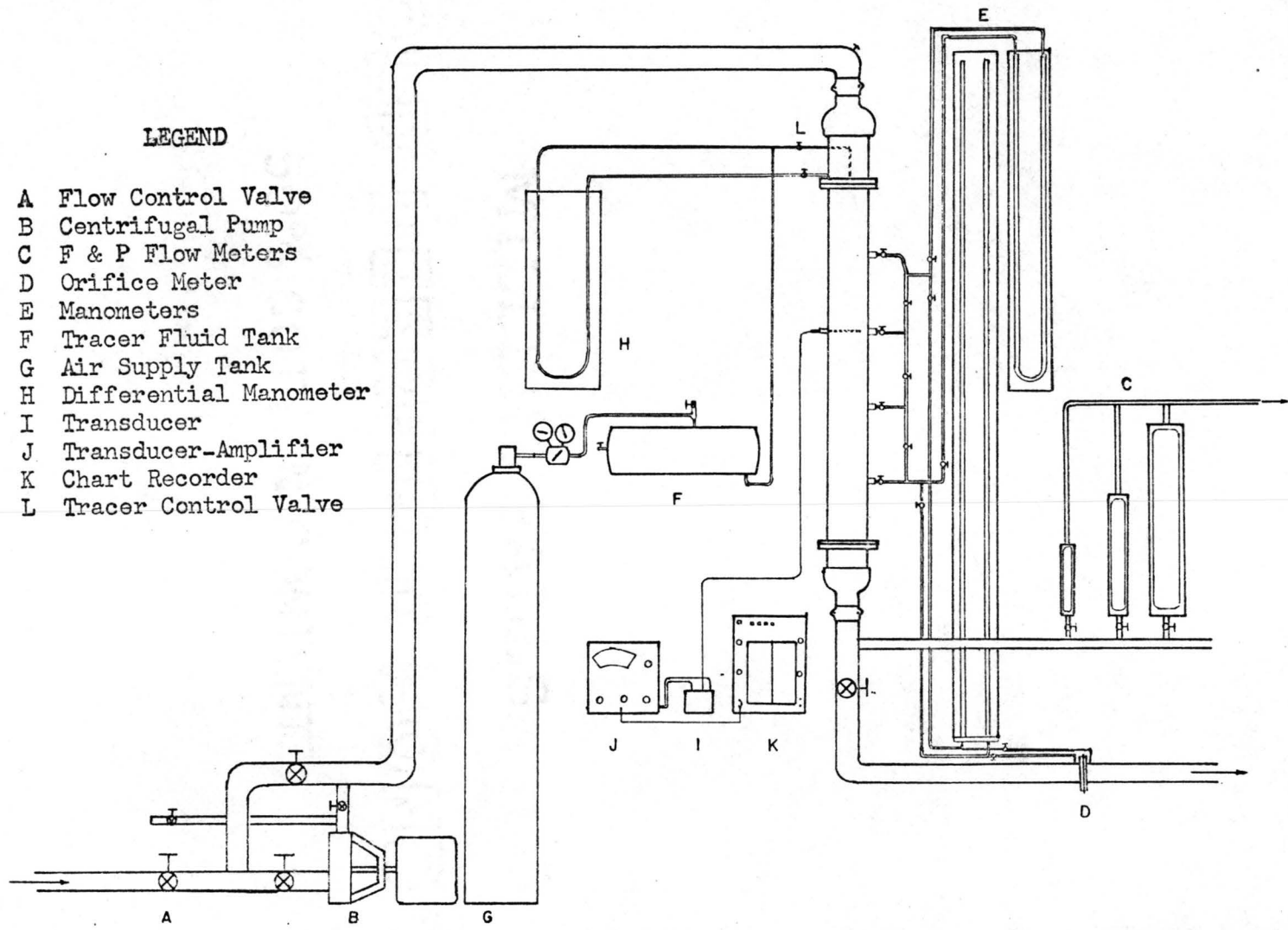
LEGEND

A   Flow Control Valve
B   Centrifugal Pump
C   F & P Flow Meters
D   Orifice Meter
E   Manometers
F   Tracer Fluid Tank
G   Air Supply Tank
H   Differential Manometer
I   Transducer
J   Transducer-Amplifier
K   Chart Recorder
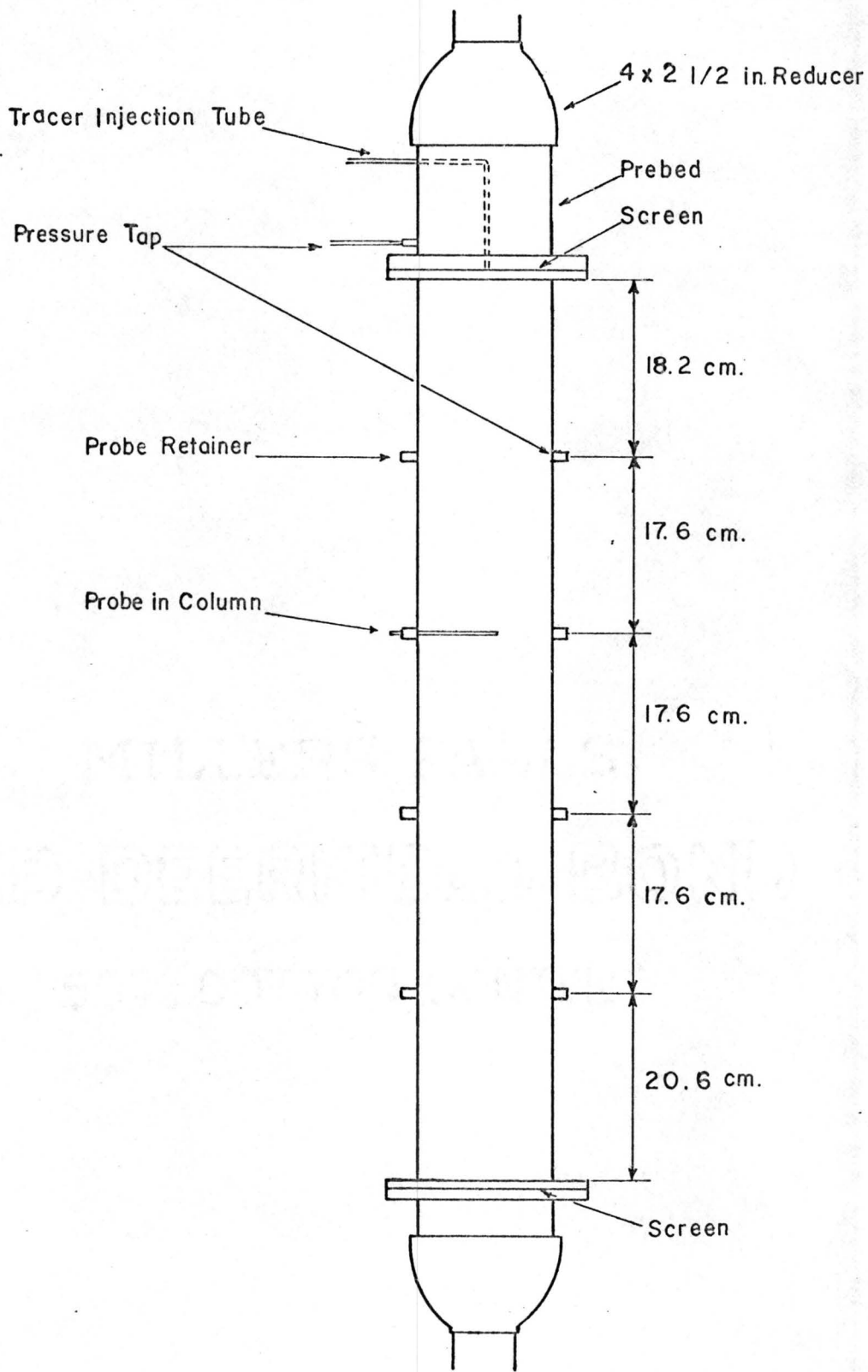L   Tracer Control Valve

Figure 4. Laboratory Apparatus

Figure 5. Details of Plexiglas Test Column

The tracer fluid is injected into the test column at z = r = 0. The tracer fluid is stored in the pressurized tank F. The tank F is kept at a constant pressure through the use of a pressure regulator in the line between the large air cylinder G at an initial pressure of 2100 psi. The pressure in tank F is set by adjusting the pressure regulator until the differential mercury manometer H is exactly balanced. The right leg of the manometer H is connected to a pressure tap in the pre-bed section one inch above the tip of the injection tube. The left leg is connected to the injection line where it enters the pre-bed section. When the differential manometer H is balanced, the tracer will flow at a steady but very low rate. When small pressures are involved as with low velocities, a very sensitive pressure regulator is used to insure that the tracer flow rate is constant. This regulator has a range of 0. psi to about 8. psi while the larger regulator has a range of 0. psi to 250 psi.

The test column containing the porous medium is a 10.0 cm. diameter by 91.5 cm. length of clear Plexiglas tube (See Figure 5). The pre-bed section is a 21. cm. length of 4 in. steel pipe packed with a uniform gravel to insure a uniform velocity profile at the entrance of the test column. A copper screen and a perforated Plexiglas plate separate the gravel in the pre-bed from that in the test column. The transition between the 2.5 inch supply line and the 4 inch pre-bed is accomplished with a standard 2.5 inch by 4 inch threaded steel reducer.

The 10. cm. diameter test column was chosen to eliminate the effect of the column wall on the flow. Franzini (8) found that the ratio of column diameter to particle diameter should be about 40. to prevent wall interference. Schwartz and Smith (18) found that this

same ratio should be 40. to insure that the average velocity along any radius across the test column is constant. As an example, they found when the ratio was 16. that the average velocity at the centerline was 0.79 of the average velocity calculated with flow meters. For this investigation, the minimum value of the ratio was 36.

The Plexiglas test column has four positions as indicated in figure 5 for the placement of the conductivity probes. The probes are made of 0.25 inch Plexiglas rod. A hole is drilled perpendicular to the rods length and a 0.06 inch diameter platinum wire is placed in it and epoxied into place. The rod is turned 90° and a 1/32 inch slot is machined through the rod and wire. The two cut faces of the platinum wire serve as electrodes. The outside ends of the platinum wire are connected to fine copper wires which are imbedded in grooves along the rod. The machined slot is filled with epoxy to leave a 1/4 inch long slot. Figure 6 shows the details of a conductivity probe.

This particular design was found by Shamir (19) to work well because it did not allow sand grains to fall between the electrode faces and it retained its shape. Both of these factors are necessary so that the electrical field does not change. This design also allowed the platinum electrode to be centered on the test column center line.

The platinum electrodes were coated with platinum black to increase the time response and stability. This was done by dipping the electrode end of the probe in a platinum chloride solution with the probe as the positive pole while a 20 volt D.C. current was applied to the solution for 30 seconds.

The tracer fluid used in this study is a sodium chloride solution with a concentration of 0.2 per cent by weight. A common method of

Solder Connection   Groove for Copper Wire   1/4"

Two Wire Shielded Cable

Retainer   Platinum Wire

1/32" Slot

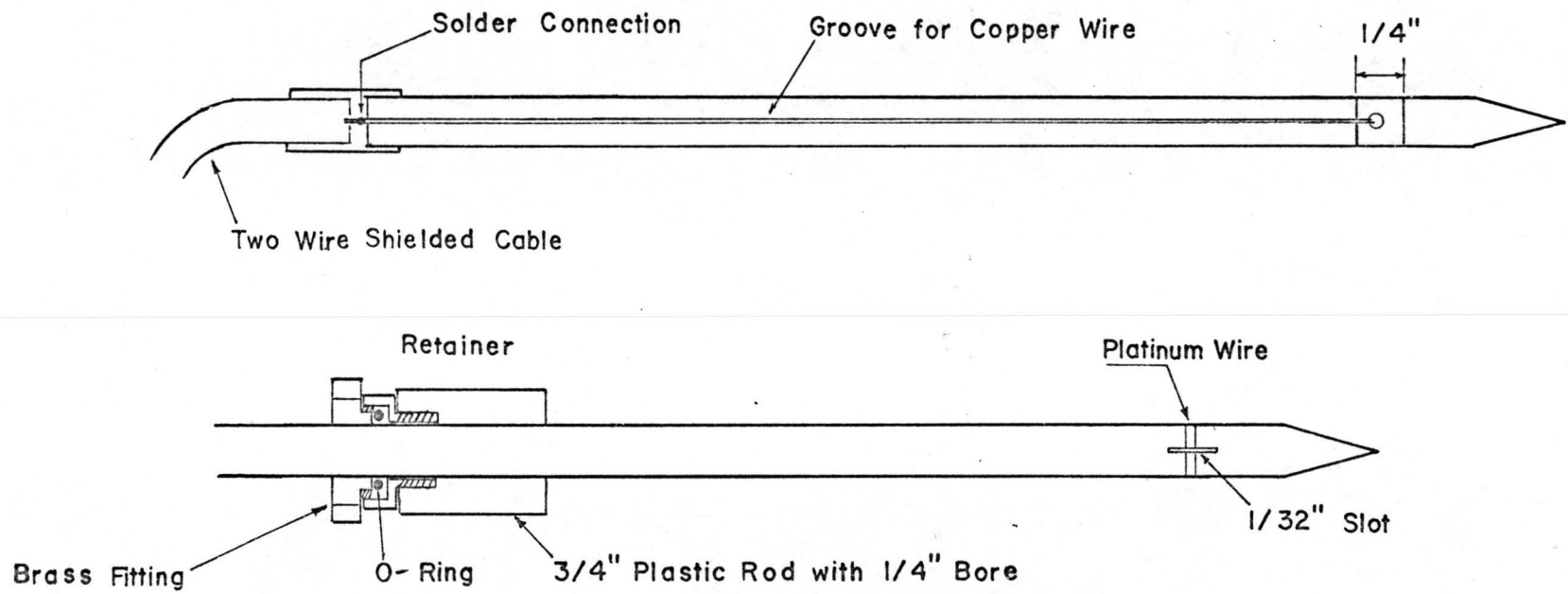Brass Fitting   O- Ring   3/4" Plastic Rod with 1/4" Bore

Figure 6. Details of Conductivity Probe

measuring the concentration of a salt in water is its electrical conductivity. This method is valid since the relationship between conductance and concentration is linear for low concentrations. Conductivity is very sensitive to temperature change so the water temperature must be constant to achieve accurate results.

In this study, the only need is relative change in concentration and not actual concentration. Since conductivity is the reciprocal of resistance, a measure of change in concentration is the change in resistance of the conductivity probe. The conductivity probe can be made a part of a resistance bridge so that when the probe resistance changes, it unbalances the bridge. This bridge unbalance causes a change in the signal from the bridge which can be interpreted as a change in concentration.

The resistance bridge is shown in figure 7. In this case, the bridge is just a transducer and will be called that hereafter. The transducer I is made of 1.0 per cent precision resistors and is built into a metal box with jack plugs to receive excitation and transmit signals.

The transducer receives its excitation from a Hewlett-Packard Transducer-Amplifier, J. The excitation is 4.5 volts at a frequency of 2400 cycles per second. The signal from the transducer can be adjusted so that the meter on the Transducer-Amplifier reads zero when fresh water is flowing through the test column. The Transducer-Amplifier has an output jack plug with a D.C. signal corresponding to the meter deflection. Since concentration versus time is needed for evaluation of D_L, the meter deflection corresponding to change in concentration must be recorded as a function of time. This is done by connecting the
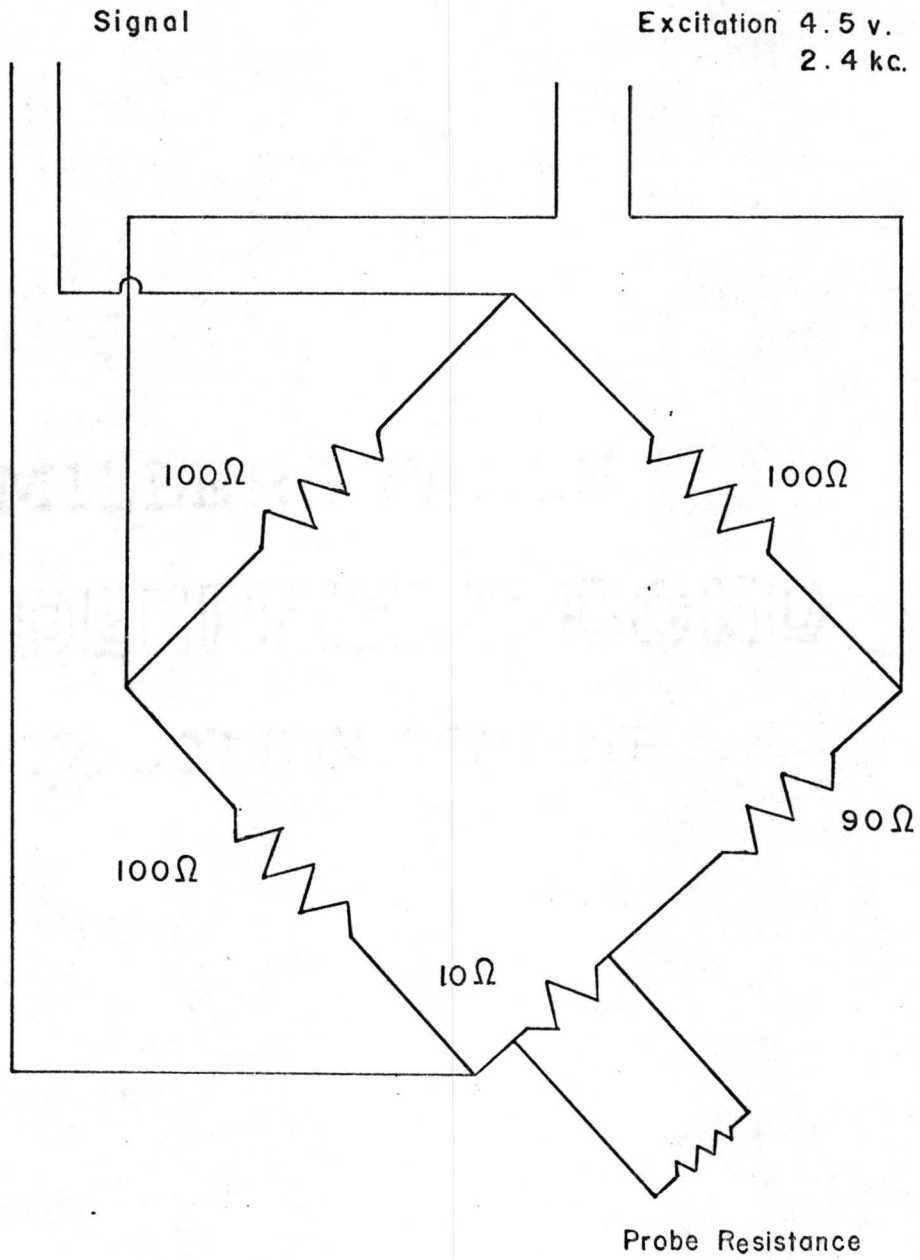
Figure 7. Resistance Bridge

output plug on the Transducer-Amplifier to a Brush Mark II chart recorder, K. The chart recorder has chart speeds of 1, 5, 25, and 125 mm/sec. Using the chart recorder, the concentration versus time curve or breakthrough curve can be obtained directly with the deflection of the chart recorder pen corresponding to concentration. A typical curve is shown in figure 8.

Laboratory Procedures

Two sizes of Poudre River sand were used in this study. The sand was sorted using a mechanical sieve shaker. All sieves were U. S. Sieve Series / ASTM Specification E-11-61. One size of sand was that which passed a no. 6 sieve but was retained on a no. 8 sieve with a mean particle diameter d_p of 2.82 mm. The other size was that which passed a no. 8 sieve but was retained on a no. 10 sieve with a mean particle diameter d_p of 2.19 mm.

The sand was packed using a 3/4 inch tamping rod. The test column was filled by putting in a 3 inch layer at a time then tamping the layer 50 times. The total weight of the clean sand used to fill the test column was recorded so that porosity could be calculated. The homogeneity of the sand pack was measured using the four pressure taps. After the sand column was saturated and a moderate flow had been established, the pressure drop between each two succeeding taps was measured with the water column manometer. If the three pressure drops were within 5 per cent, the column packing was considered homogeneous for flow in the z-direction.

The test column was saturated initially by filling it from the bottom and allowing the rising air to escape from an air release valve
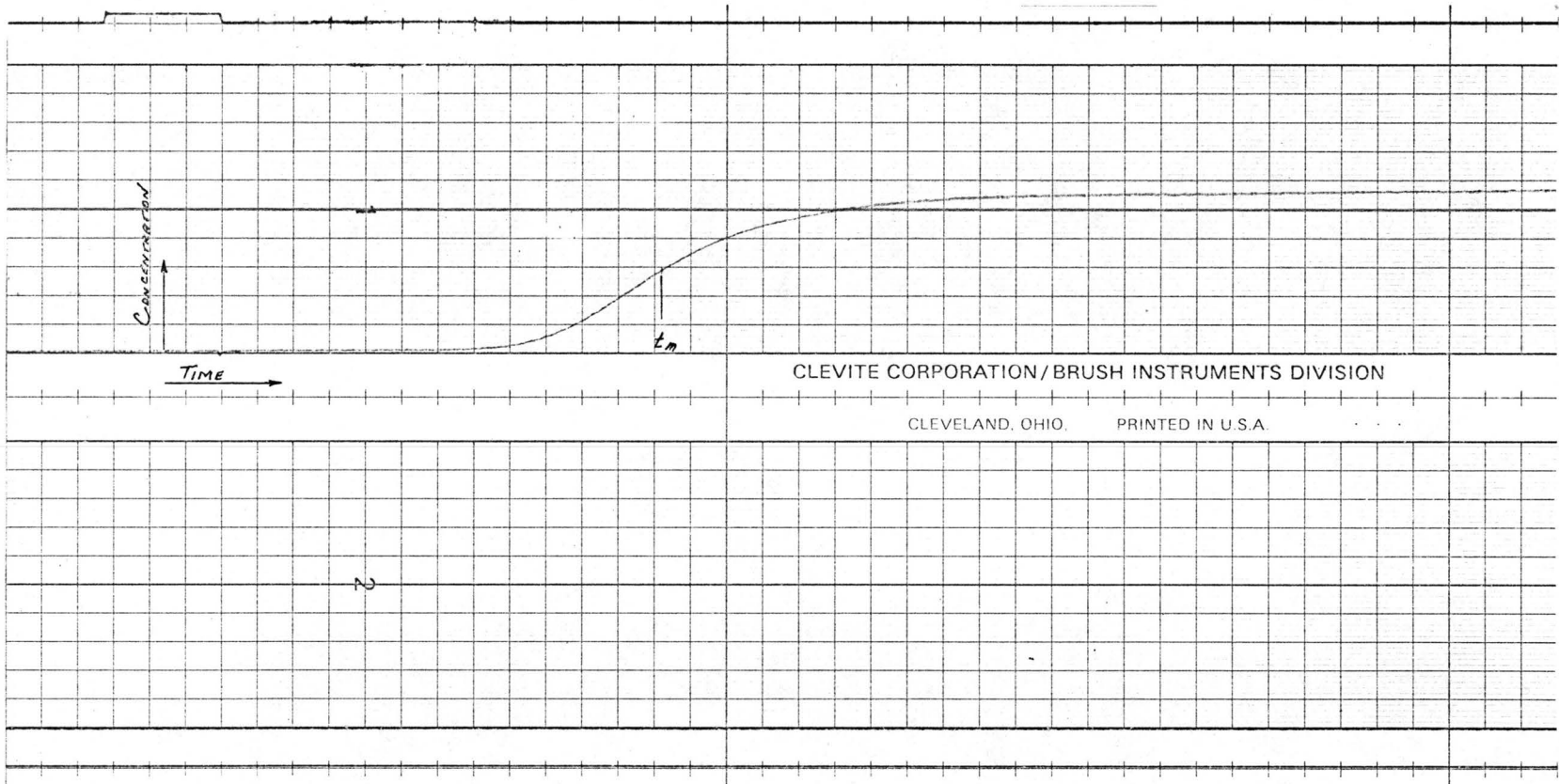
Figure 8.   Breakthrough Curve from Chart Recorder

near the top of the column. Flow was then reversed and allowed to run at least 12 hours under a moderate flow before testing began.

The tracer fluid was prepared just before testing began. The water used with the sodium chloride was the water flowing in the test column. This was done to insure that the only difference between the two miscible fluids was due to the salt added. Testing was always done in a three hour period or less. Before the next testing began, the tracer fluid was changed to insure that the temperature difference between the two fluids was minimal.

Temperature measurements were made to insure that temperature change did not affect the results. It was found that the temperature slowly changed 6° centigrade in a 2 1/2 month period.

After the tracer solution was in its tank F, the flow rate was set and allowed to reach a steady state. The Transducer-Amplifier was balanced to zero after the flow rate was set. This insured that the difference between runs was due only to dispersion. After this the flow meter was read, the differential manometer H was balanced using the pressure regulator, and the chart recorder was turned on.

Now the run was ready to begin, the quick throw valve L was opened allowing the tracer solution to begin flowing into the test column. The valve L was connected on an event marker on the chart recorder which made a blip on the edge of the chart paper when the valve L was opened or closed. The injection was allowed to continue until the deflection of the chart recorder was a constant value then the valve L was turned off. The chart recorder paper speed was set so that the slope of the breakthrough curve at the midpoint was less than 45°.

The pressure drop data was taken independent of the dispersion data. The pressure drop between two particular taps was recorded along with the flow rate. The pressure drop in centimeters of water was divided by the distance between the taps to give the hydraulic gradient ϕ .

Chapter V

CONCLUSIONS AND RECOMMENDATIONS

The experimental breakthrough curves were analyzed using equation
49. Two or more calculations were made for each curve and the values
of D_L averaged to give the final value of D_L. The calculated value of
the longitudinal dispersion coefficient D_L was recorded with the average
velocity $\bar{w}$.

Figure 9 is the log-log graph of longitudinal dispersion coef-
ficient D_L versus the average velocity $\bar{w}$. It can be seen that D_L is
not proportional to a constant power of $\bar{w}$ for the range of velocities
in this investigation. For both sand sizes there is a definite change
in slope at an average velocity $\bar{w}$ of approximately 2 cm/sec which is
in the transitional flow regime. For velocities $\bar{w}$ less than 1 cm/sec,
the relation between D_L and $\bar{w}$ is

$$D_L = a\bar{w}^{1.40} \quad .$$

For velocities $\bar{w}$ greater than 10 cm/sec, the relation between D_L and
$\bar{w}$ is

$$D_L = a\bar{w}^{0.60} \quad .$$

The larger sand size has a larger coefficient a than the smaller sand.

Figure 10 is a log-log graph of hydraulic gradient ϕ versus
average velocity $\bar{w}$. Sunada (21) and Ahmed (1) have shown that this
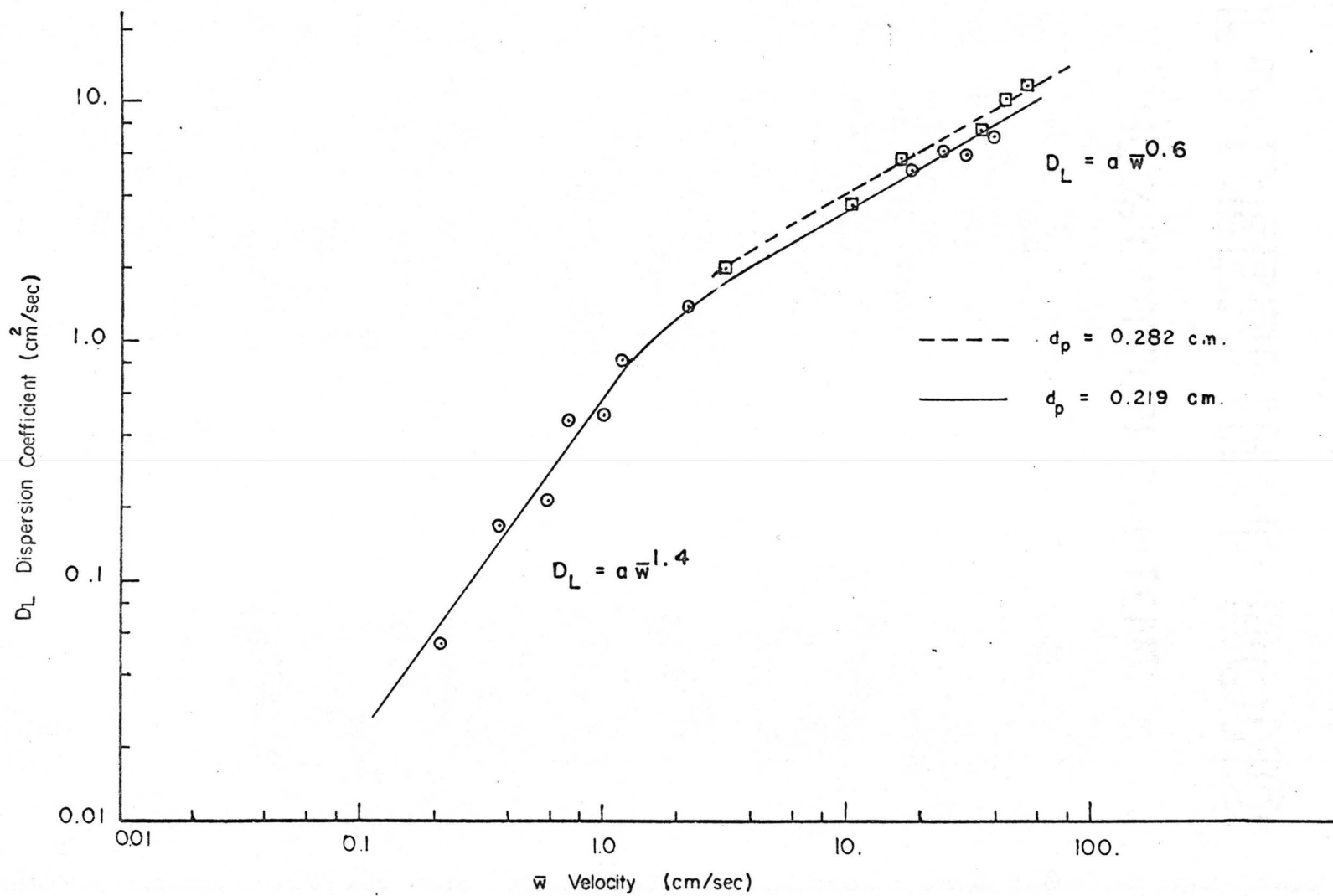
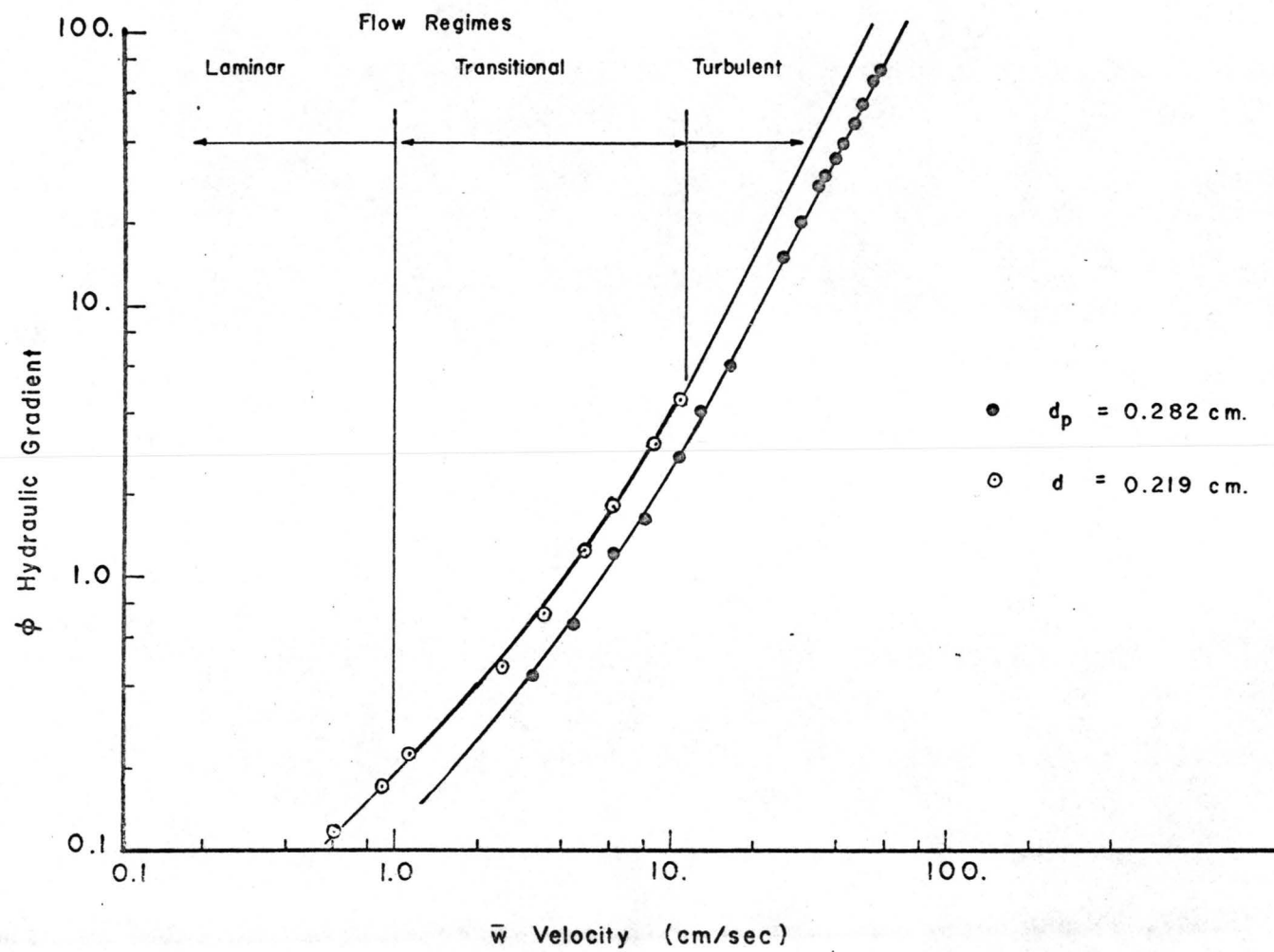Figure 9.   Longitudinal Dispersion versus Average Velocity

Figure 10. Hydraulic Gradient versus Velocity

graph indicates the regime of flow is for a particular velocity $\bar{w}$.
If the hydraulic gradient ϕ is proportional to the average velocity $\bar{w}$,
the regime of flow is laminar. If the hydraulic gradient ϕ is propor-
tional to the average velocity $\bar{w}$ squared, the regime of flow is non-
linear or turbulent.

The results of this investigation indicate that the longitudinal
dispersion coefficient D_L is not proportional to the first power of
the average velocity $\bar{w}$ for all three regimes of flow. This may be
true for laminar flow but for turbulent flow the power of $\bar{w}$ is about
0.60. This value is not nearly as high as was expected by some inves-
tigators (9, 10, 11).

The empirical equation describing the curve in figure 9 has the
form of

$$D_L = a\bar{w} - b\bar{w}^2$$

if the whole range of velocities is considered.

There also is a direct correlation between each flow regime as
indicated by figure 10 and the power N of the average velocity $\bar{w}$ in
figure 9. The transitional regime of flow begins at a velocity of
about 1.0 cm/sec and ends at about 12 cm/sec. The power N of the
average velocity $\bar{w}$ begins to decrease at about 1 cm/sec and keeps
changing until $\bar{w}$ equals about 10 cm/sec.

For fully developed turbulent flow, the longitudinal dispersion
coefficient D_L is proportional to $(\bar{w})^{0.6}$. This result is somewhat
surprising because as turbulence sets in, one would think that mixing
in the pore volume would increase. However, as the velocity increases,
the velocity distribution across a pore volume would become more

rectangular. This would decrease the chances of a tracer fluid particle being slowed down due to the viscous boundary layer. Also for turbulent flow, the actual streamlines would be less sinuous so that the paths taken by particles of a "cluster" of tracer fluid would be of a shorter length overall. These two reasons would decrease the standard deviation of the tracer distribution which would decrease the value of D_L as compared to the value that would be expected from the laminar flow regime.

Figure 11 is a log-log graph of longitudinal dispersion coefficient D_L versus Reynolds number R.

Ebach and White (7) reported that the slope of the D_L versus Reynolds number log-log graph decreased at a value of $R \geq 80$. Their data is included in figure 11 to verify this investigation's results. Figure 11 shows a transitional change in slope beginning at R = 20 and ending at about R = 100.

Based upon the results of this investigation, the following recommendations are made:

1.) Theoretical evaluation of the dispersion phenomenon

2.) Experimental results for a larger range of velocities

3.) Greater range of porous media sizes and shapes for the study of dispersion.
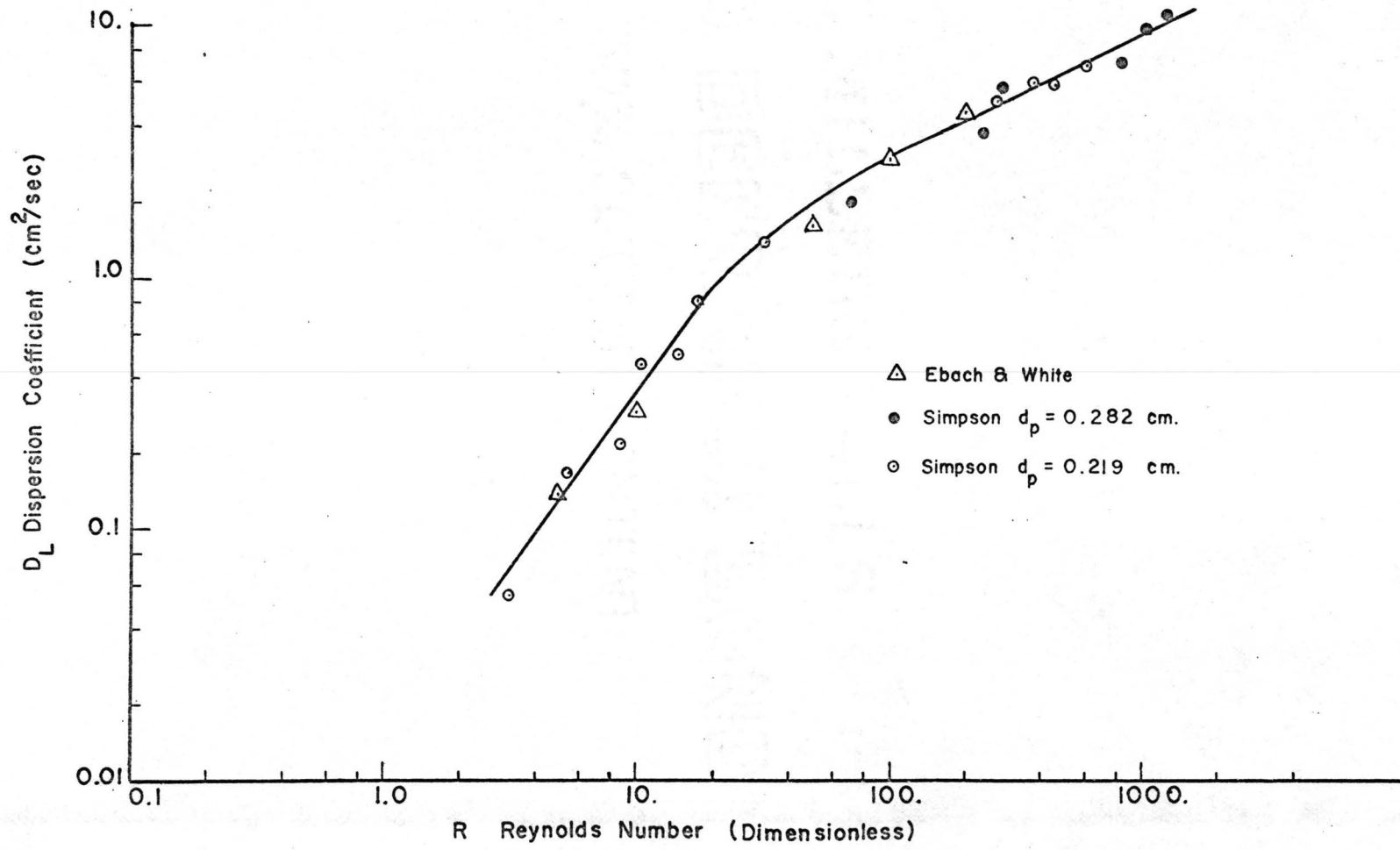
Figure 11.   Longitudinal Dispersion versus Reynolds Number

BIBLIOGRAPHY

1. Ahmed, Nazeer, Physical Properties of Porous Medium Affecting Laminar and Turbulent Flow of Water. Ph. D. Dissertation, Colorado State University, Fort Collins, 102 pp., 1967.

2. Aris, R., and N. R. Amundson, Some Remarks on Longitudinal Mixing or Diffusion in Fixed Beds. Amer. Inst. of Chem. Engs., Vol. 3, No. 2, pp. 280-282, 1957.

3. Bernard, R. A., and R. H. Wilhelm, Turbulent Diffusion in Fixed Beds of Packed Solids. Chem. Eng. Progress, Vol. 46, No. 5, pp. 233-244, 1950.

4. Crank, J., The Mathematics of Diffusion. Oxford at the Clarendon Press, Great Britain, pp. 1-5, 1956.

5. Danckwerts, P. V., Continous Flow System. Chem. Eng. Science, Vol. 2, pp. 1-13, 1953.

6. Day, P. R., Dispersion of a Moving Salt-Water Boundary Advancing Through Saturated Sand. Trans. Amer. Geophy. Union, Vol. 37, pp. 595-601, 1956.

7. Ebach, E. A., and R. R. White, Mixing of Fluids Flowing Through Beds of Packed Solids. Amer. Inst. of Chem. Engs., Vol. 4, pp. 161-169, 1958.

8. Franzini, J. B., Permeameter Wall Effect. Trans. Amer. Geophy. Union, Vol. 37, pp. 735-737, 1956.

9. Harleman, D. R. F., P. F. Mehlhorn, and R. R. Rumer, Dispersion-Permeability Correlation in Porous Media. Proc. Amer. Soc. Civil Engrs., Journal of the Hydraulics Division, Vol. 89, No. HY2, 1963.

10. Harleman, D. R. F., and J. A. Hoopes, Waste Water Recharge and Dispersion in Porous Media. Report No. 75, Hydrodynamics Lab., Dept. of Civil Eng., Mass. Inst. of Tech., 1965.

11. Kitagowa, D., Memoirs, Series A, Kyoto University, Vol. 17-18, pp. 432-441, 1934-35.

12. Klinkenberg, I. A., Residence Time Distributions and Axial Spreading in Flow Systems (with their Application in Chemical Engineering and Other Fields). Trans. Instn. Chem. Engrs., Vol. 43, 1965.

13. Miller, S. F., and C. J. King, Axial Dispersion in Liquid Flow Through Packed Beds. Amer. Inst. of Chem. Engrs., Vol. 12, pp. 767-773, 1966.

14. Parzen, E., Modern Probability Theory and Its Applications. John Wiley and Sons, Inc., New York, pp. 371-376, 1960.

15. Perkins, T. K., and O. C. Johnston, A Review of Diffusion and Dispersion in Porous Media. Soc. of Petro. Engrs. Journ., Vol. 3, pp. 70-84, 1963.

16. Rifai, M. N. E., Dispersion Phenomena in Laminar Flow Through Porous Media. Ph. D. Dissertation, University of California, Berkeley, 151 pp.

17. Scheidegger, A. E., Statistical Hydrodynamics in Porous Media. Journ. of Applied Physics, Vol. 25, pp. 994-1001, 1954.

18. Schwartz, C. E., and J. M. Smith, Flow Distribution in Packed Beds. Industrial and Eng. Chem., Vol. 45, pp. 1209-1218, 1953.

19. Shamir, U. Y., and D. F. Harleman, Numerical and Analytical Solutions of Dispersion Problems in Homogeneous and Layered Aquifers. Hydrodynamics Lab Report No. 89, Civil Eng. Dept., M. I. T., 1966.

20. Slichter, C. S., Field Measurements of the Rate of Movement of Underground Waters, Water Supply and Irrigation Paper No. 140, United States Geological Survey, 122 pp., 1905.

21. Sunada, D. K., Laminar and turbulent flow of water through homogeneous porous media. Ph. D. Dissertation, University of California, Berkeley, 71 pp., 1965.

APPENDIX A

Symbol	Description	Units
A	Constant	--
a	Constant defined where used	--
b	Constant defined where used	--
c, c_m, c_2	Concentration	M/L^2
c_o	Initial Concentration	M/L^2
D	Dispersion Coefficient	L^2/T
D_L	Longitudinal Dispersion Coefficient	L^2/T
D_R	Radial Dispersion Coefficient	L^2/T
d_p	Particle Grain Diameter	L
F	Molecular Diffusion Coefficient	L^2/T
L	Length as defined	L
n	Number of steps in random walk	--
N	Exponent	--
$p(\ )$	Probability Density Function of $(\ )$	--
$P(\ )$	Probability Distribution Function of $(\ )$	--
Pe_L	Longitudinal Peclet Number $(d_p\bar{w}/D_L)$	--
Pe_R	Radial Peclet Number $(d_p\bar{w}/D_R)$	--
R	Reynolds Number $(d_p\bar{w}\rho/\mu)$	--
r	Distance in radial direction	L
Sn	Displacement after n steps	L
t, t', t_m	Time	T

46

u, v, w	Instantaneous Velocity in x, y, and z direction, respectively	L/T
$\bar{u}, \bar{v}, \bar{w}$	Mean Velocity in x, y, and z direction	L/T
$\bar{x}, \bar{y}, \bar{z}$	Mean displacement in x, y, and z direction, respectively	L
x_i	Random displacement in random walk	L
$\alpha, \beta, \Sigma, \eta$	Variables defined where used	--
ρ	Fluid Density	M/L^3
θ	Porosity	--
ϕ	Hydraulic Gradient	--
σ	Standard Deviation	L
μ	Fluid Viscosity	$\dfrac{F\text{-}T}{L^2}$